

Complex-Formation Ability of Salicylaldehyde Thiosemicarbazone towards Zn^{II}, Cu^{II}, Fe^{II}, Fe^{III} and Ga^{III} Ions

Éva A. Enyedy,^{*[a]} Éva Zsigó,^[a] Nóra V. Nagy,^[b] Christian R. Kowol,^[c] Alexander Roller,^[c] Bernhard K. Keppler,^[c] and Tamás Kiss^[a,d]

Keywords: Solution equilibrium / Stability constants / Thiosemicarbazones / Antitumor agents / EPR spectroscopy

The stoichiometry and stability of copper(II), zinc(II), iron(II)/(III) and gallium(III) complexes of salicylaldehyde thiosemicarbazone (STSC, H₂L) have been determined by pH potentiometry, UV/Vis spectrophotometry, and ¹H NMR and EPR spectroscopy in aqueous solution (with 30% DMSO), together with the characterization of the proton dissociation processes. Mono- and bis-ligand complexes in different protonation states were identified for Fe^{II}, Fe^{III} and Ga^{III}, whereas Cu^{II} and Zn^{II} ions only form complexes with a 1:1 metal/ligand ratio. The coordination mode in the complex

[Zn₂(HL)(L)(OAc)EtOH] was confirmed by X-ray diffraction. The metal-binding ability of STSC at physiological pH is in the following order: Ga^{III} < Zn^{II} < Fe^{II} < Fe^{III} < Cu^{II}. Ga^{III}-STSC complexes show unambiguously higher stability, whereas Fe^{II}-STSC species show significantly lower stability relative to the corresponding α(N)-pyridyl thiosemicarbazones like 2-formylpyridine thiosemicarbazone or Triapine. Furthermore, the fluorescence properties of the ligand were investigated in aqueous solution, and their changes caused by complexation with Ga^{III} and Zn^{II} were studied.

Introduction

Thiosemicarbazones (TSCs) are considered to be potential therapeutics, because they possess a broad range of biological properties including antitumor, antimalarial and antimicrobial activity.^[1] The most prominent representative of this family is the α(N)-heterocyclic Triapine (3-aminopyridine-2-carbaldehyde thiosemicarbazone; 3-AP), which is currently undergoing different phase-I and -II clinical trials as an antitumor agent and demonstrates promising activity mainly in hematological malignancies.^[2] Triapine is a very strong inhibitor of ribonucleotide reductase (RNR), the rate-determining enzyme in the supply of deoxyribonucleotides for DNA synthesis required for cell proliferation. The mechanism of action involves most probably the formation of an iron(II)-Triapine complex, which reacts with molecular oxygen to result in the generation of reactive oxygen species (ROS). Subsequently, these ROS are responsible for

the quenching of the active-site tyrosyl radical of the RNR required for the enzymatic activity.^[2,3] As a result, the coordination chemistry of iron complexes of TSCs has been receiving considerable attention recently.^[4-6] Generally, the TSCs coordinate to the metal centre by means of an (N,S) bidentate mode, and when an additional coordinating group is present more diversified binding modes can occur such as the typical tridentate (X,N,S) coordination fashion.^[7] The stability of the metal complexes formed with the TSCs strongly depends on the character of the metal ion, the X-donor atom of the additional functional group and the position and type of the substituents at the TSC backbone, as has been shown in our previous papers in the case of several α(N)-pyridyl-type TSCs.^[6,8] The presence of a phenol OH group at a chelatable position like in the salicylaldehyde (or 2-hydroxybenzaldehyde) thiosemicarbazone (STSC, H₂L; Scheme 1) instead of the pyridyl nitrogen atom might provide a different and more favourable coordination for harder metal ions that prefer oxygen donor atoms. Numerous metal complexes of STSC and its derivatives with, for example, Pd^{II}, Zn^{II}, Cu^{II}, Ni^{II} and V^{IV/V} ions were prepared^[9-11] and tested in vitro on various cancer and tuberculosis cell lines, as well as parasites and pathogenic bacteria.^[10] For example, a monomeric Cu^{II} complex of STSC showed distinct activity on a human leukemia cell line^[12] and Zn^{II} complexes of various derivatives of STSC display considerable antimicrobial activity.^[13] In comparison, the STSC ligand alone possesses only low antiproliferative activity on tumor cells.^[12,14] In general, it is observed that the biological activity of the complexes of this kind of TSCs is often higher than that of the corresponding metal-

[a] Department of Inorganic and Analytical Chemistry, University of Szeged,

Dóm tér 7, 6720 Szeged, Hungary

Fax: +36-62-420505

E-mail: enyedy@chem.u-szeged.hu

Homepage: <http://www.staff.u-szeged.hu/~enyedy/Eng-CV.html>

[b] Institute of Molecular Pharmacology, Research Centre for Natural Sciences,

Hungarian Academy of Sciences,

Pusztaszeri út 59-67, 1025 Budapest, Hungary

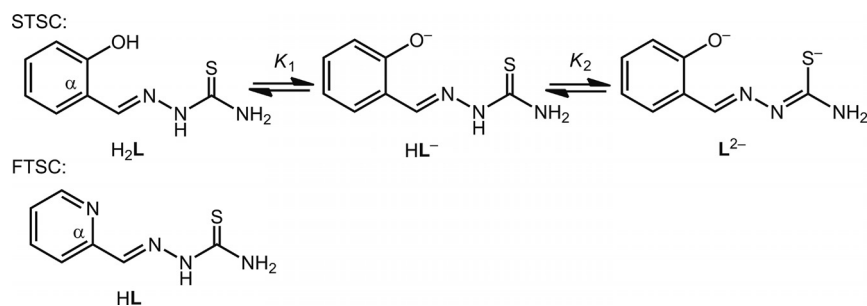
[c] Institute of Inorganic Chemistry, University of Vienna,

Währinger Strasse 42, 1090 Vienna, Austria

[d] Bioinorganic Chemistry Research Group of the Hungarian Academy of Sciences, University of Szeged,

Dóm tér 7, 6720 Szeged, Hungary

Supporting information for this article is available on the WWW under <http://dx.doi.org/10.1002/ejic.201200360>.



Scheme 1. Formulae of the ligand salicylaldehyde thiosemicarbazone (STSC, H_2L) with its deprotonation steps and 2-formylpyridine thiosemicarbazone (FTSC, HL) as a prototype of the $\alpha(N)$ -pyridyl thiosemicarbazones.

free ligands. Also noteworthy are the analytical applications of the STSC complexes for the determination of the metal content of biological samples under highly diluted conditions by spectrophotometry or fluorimetry.^[15] To gain further insight into the coordination chemistry of thiosemicarbazone ligands, thermodynamic data such the stability constants are also needed, which help in optimizing analytical or biological applications of their metal complexes.

The characterization of the potentially active complexes is usually performed in the solid phase or in a solution of organic solvents, but these techniques may not provide sufficient information on the biotransformations of metal-containing drugs in the biological fluids. However, knowledge of the speciation and the most plausible chemical forms of these complexes in aqueous solution, especially at physiological pH, is a mandatory prerequisite for understanding the mechanism and might be useful for the design of more effective and selective chemotherapeutics. Very little information is available in the literature about the thermodynamic stability of the complexes of STSC and its derivatives, most probably due to their generally low water solubility, which results in experimental limitations for solution equilibrium studies. The use of mixed organic solvent/water mixtures can provide stability information, which is undoubtedly useful for comparing the stability of complexes of different metal ions or a series of ligands. Thus, the conclusions cannot be directly transferred to the solution be-

haviour of the metal complexes in water. However, it was found in our previous work that the speciation is comparable in the presence of 30% dimethyl sulfoxide (DMSO) and pure water.^[6]

In the present work, detailed pH-potentiometric, UV/Vis spectrophotometric, EPR, 1H NMR spectroscopic and spectrofluorimetric measurements have been performed to investigate the stoichiometry and stability of the complexes of STSC formed with Fe^{II} , Fe^{III} , Cu^{II} , Zn^{II} and Ga^{III} ions in a water/DMSO mixture in addition to the proton-dissociation processes of the ligand. As the simplest tridentate O,N,S-type TSC, STSC was chosen as a model compound to clarify the stability order of the complexes of the different metal ions relative to the behaviour of $\alpha(N)$ -pyridyl-type TSCs.

Results and Discussion

Proton-Dissociation Processes and Lipophilicity

The proton-dissociation processes of STSC (shown in Scheme 1) were monitored by pH potentiometry, UV/Vis spectrophotometry and spectrofluorimetry as well as 1H NMR spectroscopic titrations. These studies were performed in 30% (w/w) DMSO/ H_2O solvent mixture due to the low solubility of the compound in pure water. The hydrolytic stability of the ligand was monitored by a second

Table 1. Proton dissociation constants (pK_a) of the ligand STSC determined by various methods;^[a] λ_{max} and molar absorptivity [$M^{-1}cm^{-1}$] values for the ligand species $[H_2L]$, $[HL]^-$, $[L]^{2-}$ determined by UV/Vis spectrophotometric titrations and calculated chemical shift [ppm] values for species of $[H_2L]$, $[HL]^-$ obtained by 1H NMR spectroscopic titrations. [$t = 25.0$ °C, $I = 0.10$ M (KCl) in 30% (w/w) DMSO/ H_2O].

	pH-metry	UV/Vis	Fluorimetry	Fluorimetry ^[b]	1H NMR spectroscopy ^[c]
pK_1	8.89(0.04)	8.84(0.05)	8.92(0.02)	8.88(0.02)	9.09(0.09)
pK_2	12.59(0.05)	12.57(0.05)	–	–	–
λ_{max} (e)					
$[H_2L]$			302 nm ($17400 M^{-1}cm^{-1}$); 328 nm ($18700 M^{-1}cm^{-1}$)		
$[HL]^-$			296 nm ($13950 M^{-1}cm^{-1}$); 373 nm ($11700 M^{-1}cm^{-1}$)		
$[L]^{2-}$			296 nm ($10760 M^{-1}cm^{-1}$); 372 nm ($15690 M^{-1}cm^{-1}$)		
δ [ppm]	CH(=N) (s)	CH(6) (d)	CH(4) (dd)	CH(5) (dd)	CH(3) (d)
$[H_2L]$	8.34	7.71	7.38	7.02	6.98
$[HL]^-$	8.42	7.69	7.15	6.51	6.60

[a] Uncertainties (SD) are shown in parentheses. [b] Determined by fluorimetric titrations in pure water. [c] Determined in 30% (w/w) $[D_6]DMSO/H_2O$.

titration with KOH from pH = 2 to 12.5 following back-acidification of the initially titrated sample. The recorded titration curves were almost exactly superimposed, therefore the protonation constants calculated from the two consecutive titrations were found to be equal within ± 0.05 log units, which indicated that no decomposition occurred. According to the literature, the neutral and completely protonated STSC (H_2L) ligand is present in the hydroxy (OH)-thione (NHC=S) form in the solid state,^[16] and the similar tautomeric form of a methoxy derivative of STSC was found in solution.^[17] Thus, two proton-dissociation processes of STSC could be determined by pH potentiometry and UV/Vis spectrophotometry. The pK_a values are collected in Table 1.

The proton-dissociation processes overlap. However, pK_1 can presumably be mainly attributed to the deprotonation of the phenol OH group, whereas pK_2 belongs largely to the hydrazine N^2-H group of the thiosemicarbazide moiety, and the negative charge is mainly localized on the S atom by means of the thione/thiol tautomeric equilibrium as shown in Scheme 1. It is noteworthy that pK_2 has a rather high value, which results in limitations to its accurate determination, because this deprotonation takes place in a pH range in which the pH measurement becomes uncertain. In the literature, values of $pK_1 = 9.67$ and $pK_2 = 11.55$ were obtained for STSC in a 50% methanol/water mixture with a similar assignment of the protons.^[18] In comparison, the proton-dissociation constant of the azomethine nitrogen atom (pK_2) is higher by more than one order of magnitude than that of the corresponding $\alpha(N)$ -pyridyl TSCs such as 2-formylpyridine TSC (FTSC; Scheme 1) ($pK_a = 11.13$).^[6] The higher electron density on the phenolate most likely results in a decrease in the acidity of the hydrazine nitrogen atom through the conjugated electron system.

The UV/Vis spectra of STSC show characteristic pH-dependent changes of the overlapping $\pi \rightarrow \pi^*$ and $n \rightarrow \pi^*$ transition bands, which originate mainly from the azomethine chromophore ($\lambda_{max} \approx 302$ nm) and the phenol moiety ($\lambda_{max} \approx 328$ nm) (Figure 1).

The spectra reveal the development of a strong band with $\lambda_{max} = 373$ nm and a decrease of the peak with $\lambda_{max} = 328$ nm in the pH range of the first deprotonation process when the ring hydroxy group releases the proton, whereas the deprotonation of the hydrazine N^2-H moiety at a pH > 11 results in less considerable changes. Proton-dissociation constants and the spectra of the individual ligand species (H_2L , HL^- , L^{2-}) (Table 1) were calculated on the basis of deconvolution of the pH-dependent UV/Vis spectra. The pK_a values are in a reasonably good agreement with those obtained by pH potentiometry. Concentration distribution curves of STSC calculated with the help of the pK_a values, together with the absorbance values at $\lambda = 373$ nm as a function of pH, are shown in Figure 1.

STSC, as with the TSCs generally, possesses intrinsic fluorescence properties as shown in the 3D spectrum in Figure 2; two excitation maxima at 320 and 390 nm are found. This can enable, for example, the monitoring of the cellular uptake or intracellular distribution of the ligand or its metal

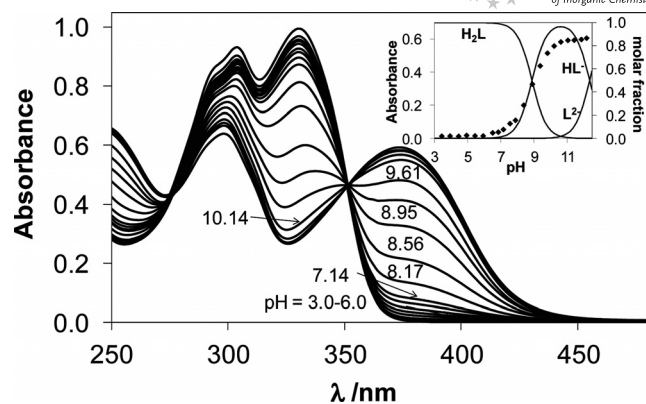


Figure 1. UV/Vis absorption spectra of the STSC ligand recorded at different pH values. Inset: concentration distribution curves for ligand species with the pH dependence of absorbance values at 373 nm (\blacklozenge) [$c_{\text{ligand}} = 50 \mu\text{M}$; $t = 25.0 \text{ }^\circ\text{C}$, $I = 0.10 \text{ M}$ (KCl) in 30% (w/w) DMSO/ H_2O].

complexes by fluorescence microscopy. The pH-dependent fluorescence spectra for STSC reveal that the emission intensity is strongly sensitive to the pH. The first proton-dissociation process primarily results in a significant increase in the intensity (Figure 2). At the highly basic pH range, at which the second dissociation takes place, the quenching effect of the hydroxide ion disturbed the measurement. Therefore, only pK_1 could be determined with appropriate accuracy by this method, and similar spectral changes and the proton-dissociation constant were also obtained in the absence of DMSO in pure water (Table 1). It is worth noting that the pK_1 values obtained for the phenol OH group in the two kinds of solvent differ practically within the experimental error; however, in the presence of DMSO a somewhat higher pK_a would be expected as is generally seen for the anionic bases.^[19]

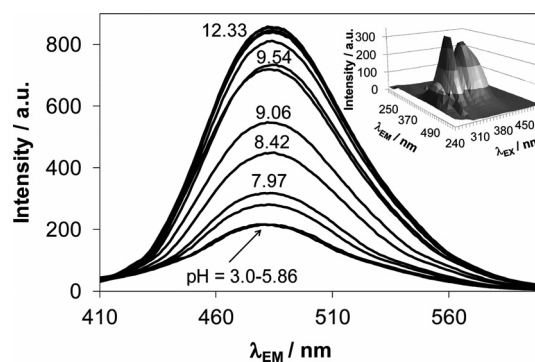


Figure 2. Fluorescence emission spectra of STSC recorded at different pH values [$c_{\text{ligand}} = 5.1 \mu\text{M}$; $\lambda_{\text{EX}} = 320$ nm; $t = 25.0 \text{ }^\circ\text{C}$, $I = 0.10 \text{ M}$ (KCl) in 30% (w/w) DMSO/ H_2O ; slits: 5 nm/5 nm]. Inset: 3D fluorescence spectra at pH = 7.40.

Additionally, ^1H NMR spectroscopic titrations were performed to monitor the proton-dissociation processes of STSC. The chemical shifts (δ) of the ring and $CH(=N)$ protons exhibited reasonable sensitivity to the protonation state of the ligand, as shown in Figure 3. Upon the first deprotonation step (between pH ≈ 8 and 10), upfield shifts

are observed for all the aromatic protons, whereas the CH(5) and CH(3) protons were found to be the most sensitive ones, and the chemical shift of the CH(=N) proton increases slightly as the pH is elevated. On the basis of these changes, pK_1 and chemical shifts of the individual ligand species (H_2L ; HL^-) were calculated (Table 1). Further minor changes were observed at $pH > 11$, which did not provide the accurate determination of the pK_2 value.

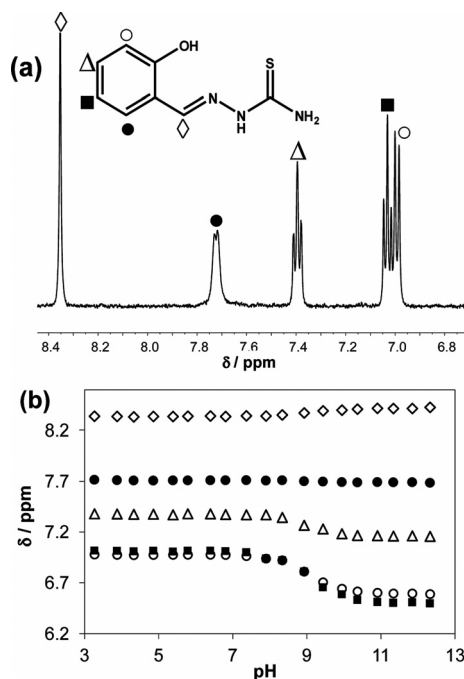


Figure 3. 1H NMR spectrum of STSC recorded at $pH = 3$ with (a) proton assignment and (b) pH dependence of the chemical shifts of the various protons of the ligand: CH(=N) (s, \diamond); CH(6) (d, \bullet); CH(4) (dd, Δ); CH(5) (dd, \blacksquare); CH(3) (d, \circ) [$t = 25.0$ °C; $I = 0.10$ M (KCl) in 30% (w/w) $[D_6]DMSO/D_2O$].

According to the pK_a values of STSC, it can be noted that the ligand is mainly neutrally charged at physiological pH (96% in H_2L form, 4% in HL^- form; see inset of Figure 1), thereby enabling an easier passage across the cell membrane relative to the ionic deprotonated forms HL^- and L^{2-} . The lipophilicity of a compound is often expressed

by the partition coefficient (P) of the neutral, non-ionized species. However, the pH-dependent distribution coefficient (D) represents the actual partitioning between isotropic solvents such as *n*-octanol and water under the given circumstances. As the lipophilic character of drugs is most interesting at $pH = 7.40$, $D_{7.4}$ is usually determined. The values of $\log D_{7.4} = 1.74 \pm 0.10$ and $\log D_{6.0} = 1.78 \pm 0.05$ were obtained for STSC by the traditional shake flask method ($\log D_{6.0}$ is equal to the $\log P$ of STSC, because at $pH = 6$ the neutral H_2L is present at $>99\%$). This result represents a more lipophilic character of the STSC ligand relative to Triapine, which has a $\log D_{7.4} = \log P = 0.85 \pm 0.08$ value.

Cu^{II} and Zn^{II} Complexes of STSC

The pH-potentiometric titration data obtained in 30% (w/w) DMSO/ H_2O mixture indicate that the STSC ligand is a very efficient Cu^{II} chelator since complex formation processes start at as low as $pH \approx 2$. It should be noted, however, that the Cu^{II} complexes precipitate at a metal/ligand ratio of 1:1 at $pH > 5$ at concentrations of 2 mM or higher. The stoichiometries of the Cu^{II} complexes and the cumulative stability constants that furnish the best fits to the experimental data are listed in Table 2. The data reveal the formation of complexes with only a 1:1 metal/ligand stoichiometry such as $[CuLH]^+$, $[CuL]$ and $[CuLH_2]^+$, which represents a fundamental difference from the behaviour of the $\alpha(N)$ -pyridyl TSCs that form in addition bis-ligand complexes, and the dinuclear $[Cu_2L_3]^{+}$.^[8] $[CuLH_2]^+$ can be considered a mixed hydroxido complex in which the coordinated water molecule is deprotonated [i.e., $[CuL(OH)]^+$]. Remarkably, $[CuL]$ has such a high stability that even at micromolar concentrations at physiological pH practically no dissociation takes place (Figure S1 in the Supporting Information).

Complex formation in the Cu^{II}–STSC system was monitored by UV/Vis spectrophotometric and EPR titrations. Weak d–d transition bands of the complexes were detected ($\epsilon \approx 100\text{--}200$ M⁻¹ cm⁻¹) in the 500–800 nm wavelength range, which showed characteristic changes when the pH was increased. In parallel to changes in the coordination mode of

Table 2. Stability constants ($\log \beta[M_pL_qH_r]$) for the metal complexes of the ligand STSC with some stepwise and derived constants at $t = 25.0$ °C, $I = 0.10$ M (KCl) in 30% (w/w) DMSO/ H_2O .^[a]

	Cu ^{II}	Zn ^{II} ^[b]	Fe ^{II}	Fe ^{III}	Ga ^{III}
$\log \beta([MLH])$	23.03(4)	18.34(3)	21.00(5)	22.26(2)	–
$\log \beta([ML])$	19.02(4)	12.78(1)	13.56(9)	18.68(3)	19.78(9)
$\log \beta([MLH_2])$	8.75(9)	1.81(2)	–	–	–
$\log \beta([ML_2H])$	–	–	32.35(9)	39.14(5)	39.57(9)
$\log \beta([ML_2])$	–	–	24.73(9)	34.02(4)	32.51(9)
$\log \beta([ML_2H_2])$	–	–	16.01(12)	22.72(7)	–
Fitting parameter [mL]	3.29×10^{-3}	3.11×10^{-3}	8.09×10^{-3}	4.52×10^{-3}	8.99×10^{-3}
$\log K([ML_2])$	–	–	11.17	15.34	12.73
$\log K([ML])/K([ML_2])$	–	–	2.39	3.34	7.05
$pM^{*[c]}$	13.3	7.1	8.2	8.4	6.0

[a] Uncertainties (SD) are shown in parentheses for the complexes determined in the present work. Charges of the complexes are omitted for simplicity. [b] Model with the dinuclear species: $\log \beta[Zn_2L_2H_2]^{2+} = 40.29(6)$; $\log \beta[Zn_2L_2H]^+ = 34.64(4)$; $\log \beta[Zn_2L_2] = 28.44(3)$; $\log \beta[ZnLH_2]^+ = 1.75(2)$; fitting parameter: 6.03×10^{-3} mL. [c] $PM^* = -\log(\Sigma[M_pH_r])$ at $pH = 7.4$ $c_M = 1$ μ M; M/STSC = 1:10.

the complexes, the λ_{\max} of these d-d bands is significantly decreased during the formation of [CuL] and further slightly decreased with the formation of [CuLH₁]⁻ (Figure 4).

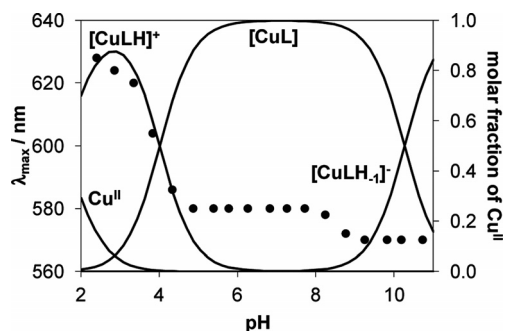


Figure 4. Concentration distribution curves of Cu^{II} complexes formed in the Cu^{II}-STSC system and pH dependence of λ_{\max} values (●) [$c_{\text{STSC}} = 1 \text{ mM}$; $M/L = 1:2$; $t = 25.0 \text{ }^\circ\text{C}$, $I = 0.10 \text{ M}$ (KCl) in 30% (w/w) DMSO/H₂O].

To elucidate the actual coordination modes and confirm the speciation model obtained by pH-potentiometry, EPR spectra were recorded at various pH values at 77 K and at room temperature. The EPR spectra recorded in frozen solution at 1:1 metal/ligand ratio could be evaluated only in the acidic region as the spectra recorded at higher pH showed a broad singlet signal that was most likely due to an aggregation of the neutral [CuL] complex formed. The isotropic values calculated by averaging the anisotropic values ($g_{\text{o,calcd.}}$ and $A_{\text{o,calcd.}}$; Table 3) are in good accordance with the corresponding values measured in solution, thus indicating that the coordination modes formed in solution are preserved upon freezing. The solution EPR spectra have been simulated simultaneously by a two-dimensional simulation that resulted in the formation constants and the individual isotropic EPR spectra (and parameters) of the complexes (Table 3). The experimental and individual spectra as well as the result of the fit are depicted in Figure 5.

The nitrogen splitting, caused by the equatorial coordination of one nitrogen atom, is well resolved in all component spectra. The deconvolution of the EPR spectra clearly shows that [CuLH₁]⁺ is the most abundant species in solution at as low as pH ≈ 2.5 –3, and the amount of free Cu^{II} ions was detected to be <10% at a 1:1 metal/ligand ratio. The complex [CuL] predominates in a wide pH range between 6 and 9, and at pH > 10 the species [CuLH₁]⁻ could be assigned in good accord with the results of pH potenti-

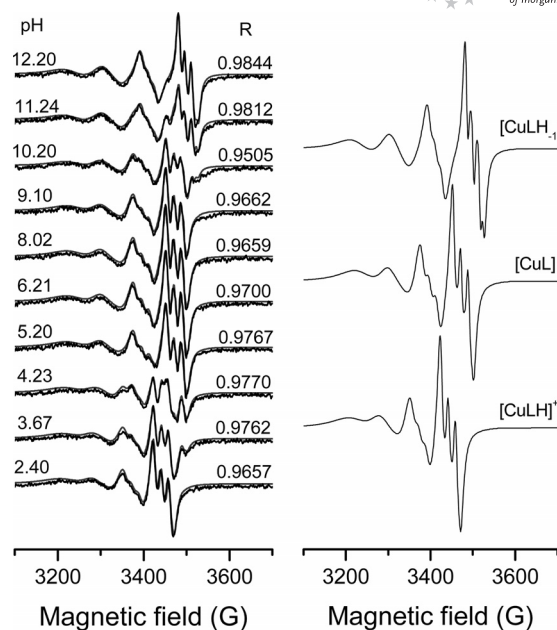


Figure 5. Experimental (black) and simulated (grey) EPR spectra of the Cu^{II}-STSC system (left side) and calculated component spectra obtained for the complexes [CuLH₁]⁺, [CuL] and [CuLH₁]⁻ (right side) [$c_{\text{STSC}} = 1 \text{ mM}$; $M/L = 1:2$; room temperature, $I = 0.10 \text{ M}$ (KCl) in 30% (w/w) DMSO/H₂O].

ometry. It is noteworthy that there was no indication for the formation of any dinuclear or bis-ligand complexes even at higher ligand excess amounts under the conditions. Numerous X-ray structures represent dinuclear Cu^{II} complexes of derivatives of STSC; however, they were crystallized from organic solvents;^[11] therefore, it is unknown if these species are stable in aqueous solution. Based on the low g_{o} and high A_{o} isotropic values, it is likely that all complexes possess tridentate coordination of the ligand and a nearly square-planar geometry. In the species [CuLH]⁺, the ligand can coordinate through the deprotonated phenol O⁻, N¹ and the thione S atoms, because the hydrazine N²-H moiety is still protonated. This coordination pattern was also found in an X-ray crystal structure of Cu^{II} and STSC^[20] and its methoxy and bromo derivatives.^[21] Deprotonation of the hydrazine N²-H group of the complex results in lower g_{o} and higher A_{o} parameters due to the increased ligand field around the Cu^{II} ion, thus the (O⁻, N¹, S⁻) binding mode is the most feasible in the species [CuL]. A further decrease in g_{o} and increase in A_{o} values supports the deprotonation

Table 3. Isotropic EPR parameters of the components obtained for the Cu^{II}-STSC system with overall stability constants of the complexes obtained from the two-dimensional simulation of EPR spectra.^[a,b]

	$\log \beta$	g_{o}	A_{o} [G]	a_{o}^{N} [G]	a [G]	β [G]	γ [G]
Cu ^{II} [c]	–	2.1970	34.3	–	51.9	–2.2	0.7
[CuLH] ⁺	23.80(3)	2.1084(1)	68.2(1)	17.4(1)	25.5(1)	–15.9(1)	3.5(1)
[CuL]	19.50(3)	2.0945(1)	73.1(1)	17.7(1)	22.9(1)	–14.1(1)	3.3(1)
[CuLH ₁] ⁻	8.8(1)	2.0891(2)	85.5(2)	15.1(3)	21.2(1)	–14.1(1)	3.0(1)

[a] Uncertainties of the last digits are shown in parentheses. [b] Anisotropic EPR parameters of [CuLH]⁺: $g_{\text{x}} = 2.054(1)$; $g_{\text{y}} = 2.035(1)$; $g_{\text{z}} = 2.2278(5)$; $A_{\text{x}} = 23(2) \text{ G}$; $A_{\text{y}} = 23(2) \text{ G}$; $A_{\text{z}} = 168(1) \text{ G}$; $a_{\text{N}_{\text{x}}} = 6(2) \text{ G}$; $a_{\text{N}_{\text{y}}} = 17.2(5) \text{ G}$; $a_{\text{N}_{\text{z}}} = 6(2) \text{ G}$; $g_{\text{o,calcd.}} = 2.1056$; $A_{\text{o,calcd.}} = 74.4 \text{ G}$. [c] Fixed values obtained from separate measurements of Cu^{II} without the ligand.

FULL PAPER

of the water molecule that coordinates in the fourth equatorial position of $[\text{CuLH}_1]^-$ ($= [\text{CuLOH}]^-$).

X-ray-diffraction-quality crystals of the dinuclear complex $[\text{Zn}_2(\text{HL})(\text{L})(\text{OAc})\text{EtOH}] \cdot \text{H}_2\text{O} \cdot 0.65\text{EtOH}$ were obtained (Figure 6) from a solution of $\text{Zn}(\text{OAc})_2$ in ethanol/water and an excess amount of STSC. The two Zn^{II} atoms are chelated by the O,N,S-donor set of an STSC ligand and bridged by the two phenolate O atoms, which leads to a Zn_2O_2 core. In addition, Zn1 is coordinated by one molecule of EtOH and Zn2 by OAc^- , thereby resulting in a distorted square-pyramidal environment of the two zinc atoms. It is worth noting that one of the zinc ions (Zn1) is chelated by L_2^- and the other one (Zn2) by HL^- . This is accompanied by a lengthened bond C8–S1A/B at 1.744(6)/1.756(6) Å for the thiolato form (L_2^-) relative to C18–S2 at 1.699(4) Å for the thione ligand (HL^-) and a shorter N1...C8 distance [2.260(4) Å] relative to N4...C18 [2.346(4) Å], which is in accord with literature parameters to distinguish between these ligand forms of TSCs.^[22] A similar coordination pattern, but with two HL^- ligands, was observed for zinc complexes of 2,4-dihydroxybenzaldehyde TSCs.^[23]

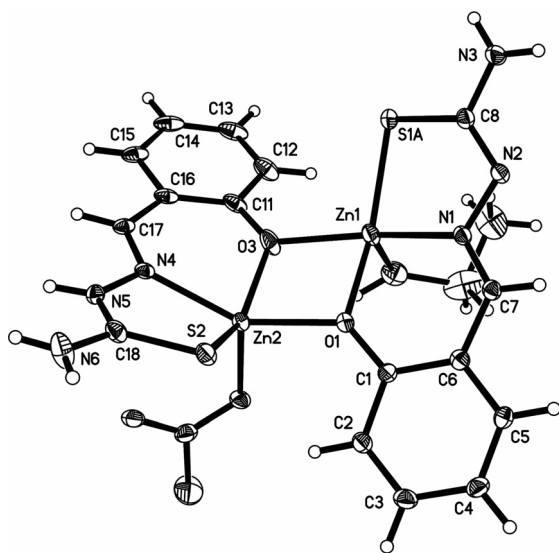


Figure 6. X-ray crystal structure of $[\text{Zn}_2(\text{HL})(\text{L})(\text{OAc})\text{EtOH}] \cdot \text{H}_2\text{O} \cdot 0.65\text{EtOH}$ with thermal ellipsoids at the 30% probability level (the co-crystallized ethanol and water molecules as well as the disorder of OAc, EtOH and S1 are omitted for clarity).

Clarifying the geometry and the actual coordination mode of the Zn^{II} complexes in solution is more difficult, because the techniques applied such as ^1H NMR spectroscopy, UV/Vis spectrophotometry and fluorimetry can mainly give information about the speciation and binding strength but have limitations in, for example, distinguishing between the formation of mononuclear and dinuclear species with the same metal/ligand ratio. Therefore, two kinds of models could be calculated on the basis of the pH-potentiometric data. One consists of the formation of only mononuclear species; whereas the other one considers dinuclear complexes (see Table 2). The latter model gave somewhat poorer fits between the experimental and calculated

titration curves; however, both models suggest that no bis-ligand complexes are formed. The pH-metric data showed that complexation of Zn^{II} with STSC proceeds only at $\text{pH} > 5$, which represents the lower stability of these complexes relative to those of Cu^{II} . This was also confirmed by the ^1H NMR spectroscopic titrations. First of all, a slow ligand-exchange process was found with respect to the NMR spectroscopic timescale as the chemical shifts of the protons of the metal-free and the bound ligand can be seen separately. Below $\text{pH} \approx 5$, only the peaks of the ligand (H_2L) can be observed. As the pH increases, a new set of very small signals appears, possibly from the complex $[\text{ZnLH}]$; these signals, slightly shifted, become predominant between $\text{pH} = 7$ and approximately 10 according to $[\text{ZnL}]$ (or $[\text{Zn}_2\text{L}_2]$ considering the second model) (Figure 7a) without any free ligand at a 1:1 metal/ligand ratio. At $\text{pH} > 10$, the peaks of the complex show a small upfield shift as the mixed hydroxido species $[\text{ZnLH}_1]^-$ is formed. When an excess amount of ligand is applied, the same set of peaks are present in the spectra, which shows the formation of the same kind of species independent of the metal/ligand ratio (yet together with the excess amount of free STSC) (Figure 7a). The distribution of the ligand between the bound and unbound fractions at a 1:2 metal/ligand ratio calculated on

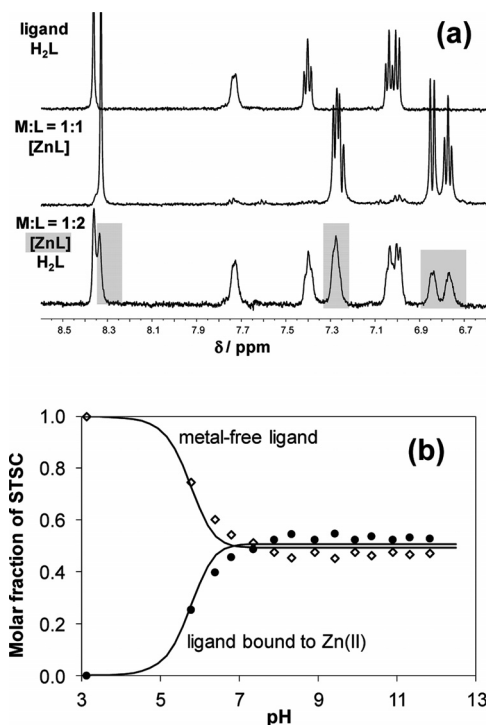


Figure 7. ^1H NMR spectra of the STSC ligand alone and the Zn^{II} -STSC system at (a) 1:1 and 1:2 metal/ligand ratio recorded at $\text{pH} = 7.4$ ($[\text{ZnL}]$ or $[\text{Zn}_2\text{L}_2]$) and (b) summed concentration distribution curves for the Zn^{II} -STSC (1:2) system (solid lines) calculated on the basis of the stability constants together with the molar fraction of the metal-free (\diamond) and bound ligand (\bullet) estimated from the integrated area of the signals of the $\text{CH}=\text{N}$ (s) protons [$c_{\text{STSC}} = 1 \text{ mM}$; $t = 25.0 \text{ }^\circ\text{C}$; $I = 0.10 \text{ M}$ (KCl) in 30% (w/w) $[\text{D}_6]\text{DMSO}/\text{D}_2\text{O}$].

the basis of the stability constants and the integrated area of the signals of the $CH=N$ (s) protons are in good agreement (Figure 7b).

Additionally, the Zn^{II} -STSC system was studied by spectrofluorimetric titrations. Out of the two excitation maxima of the ligand (see inset of Figure 2), the 320 nm excitation wavelength was used to record the pH-dependent emission spectra (Figure 8). The spectra obtained at $pH < 6$ were identical to those of the ligand alone, upon increasing the pH, a band with $\lambda_{EM} = 450$ nm appears with constant intensity between $pH = 7.4$ and 9.6. This is the pH range of the formation of the neutral complex $[ZnL]$ under these highly diluted conditions. It should be noted that the intensity of the fluorescence of this complex is roughly half of that of the metal-free ligand at physiological pH. Moreover, in accordance with the concentration distribution curves calculated with the help of the stability constants, at higher pH the formation of $[ZnLH_{-1}]^{-}$ was observed, accompanied by an increase in the wavelength of $\lambda_{EM(max)}$ and the fluorescence intensity.

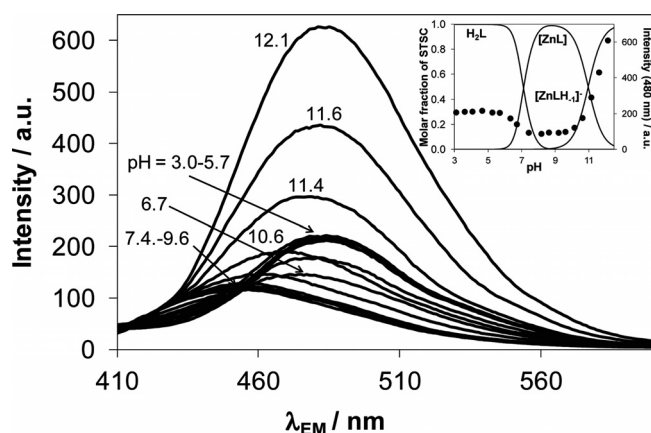


Figure 8. Fluorescence emission spectra of the Zn^{II} -STSC system. Inset: corresponding concentration distribution curves calculated with the model containing only mononuclear species and pH dependence of the intensity values at 480 nm (\bullet) [$\lambda_{EX} = 320$ nm; $c_{STSC} = 5 \mu M$; $M/L = 1:1$; $t = 25.0$ °C, $I = 0.10$ M (KCl) in 30% (w/w) DMSO/ H_2O ; slits: 5 nm/5 nm].

$Fe^{II/III}$ and Ga^{III} Complexes of STSC

The stoichiometries of the Fe^{II} , Fe^{III} and Ga^{III} complexes and the overall stability constants determined by pH potentiometry are collected in Table 2. In addition to the mono-ligand complexes (see, for example, the Cu^{II} species above for their interpretation), formation of bis-complexes such as $[ML_2H]$, $[ML_2]$ and $[ML_2H_{-1}]$ was observed. Similarly to the Cu^{II} and Zn^{II} complexes, the metal ions are tridentately coordinated by STSC: HL, with an O^-,N^1,S -donor set and with the proton presumably located at the non-coordinating hydrazine N^2 atom, and $[ML_2]$ with an O^-,N^1,S -donor set. This coordination mode was also confirmed by X-ray diffraction of the $[Fe^{III}L_2]^{-}$ complex of STSC^[24] and related ligands.^[25] Formation of complexes $[ML_2H_{-1}]$ at basic pH could be presumed by the pH-

potentiometric measurements. These complexes are possibly mixed hydroxido species in which one coordinated donor group is displaced by an OH^- ion.

Complex formation of Fe^{II} , Fe^{III} and Ga^{III} ions with STSC was additionally investigated by UV/Vis spectrophotometric measurements, in the case of Fe^{II} under strictly anaerobic conditions. Formation of the mono-ligand Fe^{II} species resulted in a shoulder in the range of 430–480 nm, whereas formation of the green bis-ligand complexes was accompanied by the development of an absorption band with a maximum at approximately 600 nm (Figure S2 in the Supporting Information). The Fe^{II} species have intense colours; however, their molar absorptivities are considerably lower than those of the $\alpha(N)$ -pyridyl TSC complexes.^[6,8] The spectrophotometric titrations with Fe^{III} confirm the predominant formation of the $[Fe^{III}L_2]^{-}$ complexes ($\lambda_{max} = 368$ nm; $\epsilon_{368nm} = 16700$ $M^{-1}cm^{-1}$) between $pH = 7$ and 9, as expected on the basis of pH-potentiometry, whereas the spectra show CT bands of the complexes strongly overlapped with the ligand bands.

Ga^{III} -STSC complexes represent relatively high stability and their $\log \beta$ values are comparable to those of the Fe^{III} species (see data in Table 2). However, Ga^{III} has a stronger tendency to hydrolyze than the corresponding Fe^{III} complexes accompanied by the formation of the water-soluble Ga^{III} -hydroxido species. The hydrolysis suppresses the presence of the Ga^{III} complexes at neutral or higher pH and considerably decreases the conditional stability constants (Figure S3 in the Supporting Information). The effect of the hydrolysis at physiological pH on the speciation of the Ga^{III} -STSC system at a 1:2 metal/ligand ratio is clearly illustrated in Figure 9. A significant amount of $[Ga(OH)_4]^{-}$ is predicted to be present at the millimolar concentration range alongside the species $[GaL_2H]$ and $[GaL_2]^{-}$, and the hydrolysis is more pronounced, if the solution is more diluted, thereby resulting in total dissociation at a concentration of as low as approximately 10 μM .

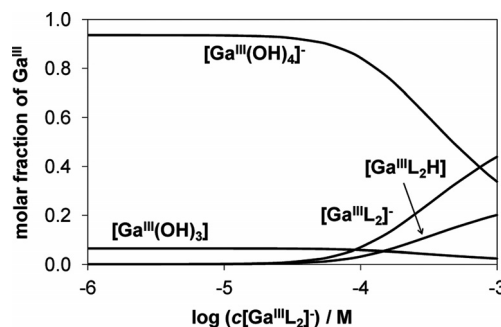


Figure 9. Representative concentration distribution diagram for Ga^{III} -STSC complexes at various total concentrations of the $[Ga^{III}L_2]^+$ complex at $pH = 7.4$ [$t = 25.0$ °C, $I = 0.10$ M (KCl) in 30% (w/w) DMSO/ H_2O].

The formation of the Ga^{III} -STSC complexes in the acidic pH range, the varying extent of hydrolysis depending on the total concentrations and the liberation of the metal-free ligand could be easily investigated by 1H NMR spec-

troscopy due to the slow ligand-exchange processes, by UV/Vis spectrophotometry through the changes of the ligand absorption bands (not shown here), and by spectrofluorimetry. The fluorimetric titrations revealed the development of a new emission maximum at 450 nm in parallel with the formation of the species $[\text{GaL}]^+$ in the acidic pH range. At higher pH, however, identical spectra to those of the metal-free ligand were observed on account of the complete complex dissociation (as illustrated in Figure 10) through the changes of the intensities at 450 nm with increasing pH.

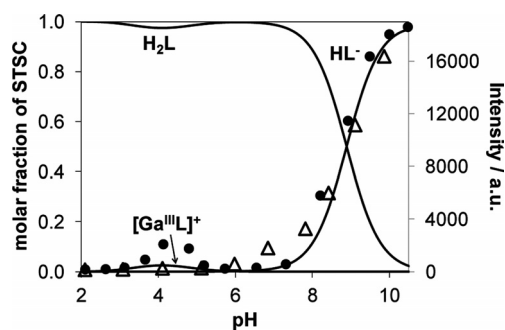


Figure 10. Concentration distribution curves of the Ga^{III} -STSC system together with the pH dependence of the intensity values at 450 nm (\bullet) and for the ligand alone (Δ) [$\lambda_{\text{EX}} = 320 \text{ nm}$; $c_{\text{STSC}} = 5 \mu\text{M}$; $\text{M/L} = 1:2$; $t = 25.0 \text{ }^\circ\text{C}$, $I = 0.10 \text{ M}$ (KCl) in 30% (w/w) DMSO/ H_2O ; slits: 10 nm/10 nm].

Comparison the Stability of the Complexes of STSC and $\alpha(N)$ -Pyridyl TSCs

Direct comparison of the stability constants of the STSC complexes formed with the different metal ions (Table 2) reveals the following stability order: $\text{Zn}^{\text{II}} < \text{Fe}^{\text{II}} \ll \text{Fe}^{\text{III}}, \text{Cu}^{\text{II}}, \text{Ga}^{\text{III}}$. It is worth noting that Cu^{II} and Zn^{II} ions form complexes only with 1:1 metal/ligand ratio, whereas the formation of bis-ligand complexes is favourable in the case of $\text{Fe}^{\text{II/III}}$ and Ga^{III} ions. However, despite the high $\log \beta$ values, there is a significant tendency of certain metal ions to hydrolyze at physiological pH, especially in the case of Ga^{III} , which results in decreased stability. As a consequence, the Ga^{III} -STSC complexes dissociate completely at concentrations $< 10^{-4} \text{ M}$ at neutral pH (see Figure 9). In contrast, $[\text{CuL}]$ does not dissociate at $\text{pH} = 7.4$ up to concentrations of at least 10^{-6} M (Figure S1 in the Supporting Information). For the most abundant species, $[\text{ZnL}]$ and $[\text{Fe}^{\text{III}}\text{L}_2]^-$, at $\text{pH} = 7.4$ almost no dissociation can be observed at millimolar concentrations, but a continuous increase of the free metal ions up to 60% Zn^{2+} and 35% Fe^{3+} (as $[\text{Fe}(\text{OH})_2]^+$) at 10^{-6} M (Figure S1) is seen. In the case of Fe^{II} , the complexes $[\text{Fe}^{\text{II}}\text{L}_2\text{H}]^-$ and $[\text{Fe}^{\text{II}}\text{L}_2]^{2-}$, which are predominant at millimolar concentrations, undergo partial dissociation during dilution through the loss of one tridentate ligand. The pM^* values have been calculated for all investigated metal ions to provide a comparable basis of the relative chelating ability of STSC at physiological pH (see Table 2; pM^* is the negative logarithm of the summed equilibrium concentrations of the free metal ion and its hy-

droxido species, thus the unbound metal fraction, under the conditions employed, unlike the generally used $\text{pM} = -\log[\text{M}]$ value, which only represents the equilibrium concentration of the free metal ion). According to these pM^* values the effectiveness of STSC to chelate a metal ion at $\text{pH} = 7.4$ is $\text{Ga}^{\text{III}} < \text{Zn}^{\text{II}} < \text{Fe}^{\text{II}} < \text{Fe}^{\text{III}} < \text{Cu}^{\text{II}}$.

STSC provides an ($\text{O}^-, \text{N}^1, \text{S}^-$) binding mode with the formation of a six- and a five-membered ring system between metal atom and ligand relative to the ($\text{N}_{\text{pyr}}, \text{N}^1, \text{S}^-$) coordination of the $\alpha(N)$ -pyridyl TSCs with two five-membered chelate rings. To clarify the effect of this difference in the binding pattern on the stability of the metal compounds, $\log \beta$ values of the corresponding complexes of STSC, FTSC and Triapine were compared on the basis of our previous publications^[6,8] (Table S1 in the Supporting Information). It is noteworthy that these $\alpha(N)$ -pyridyl TSCs have overall protonation constants $\log \beta(\text{H}_2\text{L})$ that are approximately 7 orders of magnitude lower than for STSC, which makes a direct comparison of the $\log \beta$ values of the metal complexes more difficult. However, it can be recognized easily that, for example, the species $[\text{Ga}^{\text{III}}(\text{L})_2]^-$ ($\text{H}_2\text{L} = \text{STSC}$) has a significantly higher overall stability constant than those of FTSC or Triapine, and the differences between the $\log \beta$ values are much larger than those of the protonation constants. In the case of Fe^{II} complexes, however, the stability constant of $[\text{Fe}^{\text{II}}(\text{L})_2]^{2-}$ ($\text{H}_2\text{L} = \text{STSC}$) is only somewhat higher than that of the $\alpha(N)$ -pyridyl TSCs. To indicate the ligand preferences at various pH values, predominance curves for hypothetical M -STSC-FTSC systems at equimolar ligand concentrations were calculated (Figure 11).

The higher basicity of STSC results in stronger ligand effectiveness at higher pH, and consequently the ligand FTSC is presumed to be a more powerful competitor at lower pH. Thus, in the case of Cu^{II} , Zn^{II} and Fe^{III} , in which the $\log \beta$ value is near the expected value on the basis of the difference between the protonation constants, the FTSC complexes are predominant in the acidic pH range, and those of STSC are predominant at the neutral and basic pH range (Figure 11a). In the case of Ga^{III} , the complex formation with STSC is much more favourable over the whole pH range relative to that of FTSC (and Triapine, not shown), which indicates the significantly increased stability on account of the involvement of the phenol O atom in the coordination instead of the pyridyl nitrogen atom (Figure 11b). Despite this stability-increasing effect, STSC is still incapable of protecting Ga^{III} from hydrolysis under diluted conditions at physiological pH as discussed earlier (Figure 9). In the case of Fe^{II} , the $\alpha(N)$ -pyridyl TSCs are unambiguously more efficient chelators than STSC over a wide pH range (Figure 11c). The binding to Fe^{II} is assumed to be crucial to the biological activity of TSCs through the inhibition of the RNR enzyme. Thus, the diminished stability of the Fe^{II} -STSC complexes is probably one reason for the considerably weaker activity of STSC relative to $\alpha(N)$ -pyridyl TSCs.^[13] It is important to note that terminal dimethylation of FTSC leads to remarkably stronger Fe^{II} -binding ability and higher cytotoxicity,^[4,6] therefore, a sim-

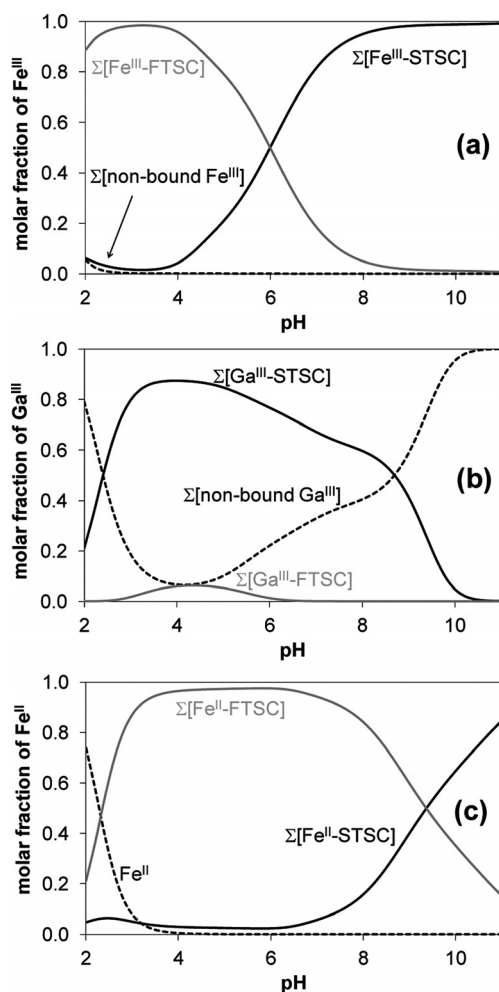


Figure 11. Predominance diagram for the hypothetical (a) Fe^{III}–STSC–FTSC. Summed equilibrium concentrations of the STSC complexes (solid black line), FTSC complexes (solid grey line) and unbound metal ion (dashed black line) [$c_M = 1 \text{ mM}$; $c_{\text{STSC}} = c_{\text{FTSC}} = 2 \text{ mM}$; $t = 25.0 \text{ }^\circ\text{C}$, $I = 0.10 \text{ M}$ (KCl) in 30% (w/w) DMSO/H₂O].

ilar derivatization is suggested for STSC-type ligands to improve their biological activity.

Conclusion

The stoichiometry and stability of the complexes of STSC formed with Cu^{II}, Zn^{II}, Fe^{II}, Fe^{III} and Ga^{III} were studied in partially aqueous solution with a focus on the most plausible species that emerged at physiological pH. On the basis of the pH-potentiometric data, it was found that Cu^{II} and Zn^{II} ions prefer the formation of complexes with 1:1 stoichiometry, whereas Fe^{II}, Fe^{III} and Ga^{III} preferentially form 1:2 metal/ligand complexes. The speciation models were confirmed by various techniques such as ¹H NMR spectroscopy, UV/Vis spectrophotometry, fluorimetry and EPR spectroscopy depending on the nature of the metal ion. In the protonated complexes ([MLH] or [ML₂H]), the (O⁻,N¹,S) binding mode with a protonated non-coordinating hydrazine N² atom is suggested, whereas (O⁻,N¹,S⁻) coordination takes place in the [ML]- and [ML₂]-type com-

plexes. The formation of mixed hydroxido species was also assumed at basic pH in the cases of Zn^{II}, Cu^{II} and Fe^{II/III}.

The predominant species at pH = 7.4 are [CuL], [ZnL], [Fe^{II}L₂H]⁻ and [Fe^{II}L₂]²⁻, [Fe^{III}L₂]⁻, [Ga^{III}L₂H] and [Ga^{III}L₂]⁻. [CuL] possesses such high stability that it is able to keep its original integrity efficiently during dilution; however, the complexes of Zn^{II}, Fe^{II}, Fe^{III} ions partially dissociate, and complete hydrolysis takes place in the case of Ga^{III} when the biologically relevant micromolar concentration range is reached. Thus, the effectiveness of STSC to chelate the metal ions at pH = 7.4 is in the order Ga^{III} < Zn^{II} < Fe^{II} < Fe^{III} < Cu^{II}.

The metal-binding ability of STSC and the composition of the complexes formed were compared with those of α(*N*)-pyridyl TSCs. Significant differences between the stoichiometry of the Cu^{II} and Zn^{II} complexes were revealed, namely, the α(*N*)-pyridyl TSCs form bis-ligand or dinuclear Cu^{II} complexes, whereas these kinds of species were not found with STSC. It was also pointed out that the coordination of the phenol oxygen atom of STSC rather than the pyridyl nitrogen atom of α(*N*)-pyridyl TSCs increases the metal-binding ability in the case of the Ga^{III} ion. However, a significantly diminished stability is shown with Fe^{II}, which is probably one reason for the lower biological activity of STSC relative to α(*N*)-pyridyl TSCs.

Experimental Section

Chemicals: Salicylaldehyde thiosemicarbazone (STSC) was purchased from Sigma–Aldrich and used without further purification. Triapine was prepared as described previously.^[4] The purity and stability of the ligands were checked, and the exact concentrations of the stock solutions prepared were determined by the Gran method.^[26] The Fe^{II} stock solution was obtained from fine Fe powder dissolved in a known amount of HCl solution under purified, strictly oxygen-free argon, then filtered, stored and used under anaerobic conditions. KSCN (Sigma–Aldrich) solution was used to check the absence of Fe^{III} traces in the Fe^{II} solution. The concentration of the Fe^{II} stock solution was determined by permanganometric titrations under acidic conditions. GaCl₃, FeCl₃, CuCl₂ and ZnCl₂ were dissolved in a known amount of HCl to obtain the Ga^{III}, Fe^{III}, Cu^{II} and Zn^{II} stock solutions, respectively. Their concentrations were determined by complexometry by means of the ethylenediaminetetraacetic acid (EDTA) complexes. Accurate strong acid content of the metal stock solutions was determined by pH-potentiometric titrations.

pH-Potentiometric Studies: The pH-metric measurements for determination of the protonation constants of the ligand STSC and the overall stability constants of the metal complexes were carried out at (25.0 ± 0.1) °C in DMSO/water (30:70, w/w) and at an ionic strength of 0.10 M (KCl, Sigma–Aldrich) to keep the activity coefficients constant. The titrations were performed with carbonate-free KOH solution of a known concentration (0.10 M). Both the base and the HCl used were Sigma–Aldrich products, and their concentrations were determined by pH-potentiometric titrations. An Orion 710A pH meter equipped with a Metrohm combined electrode (type 6.0234.100) and a Metrohm 665 Dosimat burette were used for the pH-metric measurements. The electrode system was calibrated to the pH = log[H⁺] scale in the DMSO/water solvent mixture by means of blank titrations (strong acid versus strong

base; HCl versus KOH), which is similar to the method suggested by Irving et al.^[27] in pure aqueous solutions. The average water-ionization constant, pK_w , is 14.53 ± 0.05 in DMSO/water (30:70, w/w) at 25 °C, which corresponds well to the literature data^[6,8,28] and results in $pH = 7.265$ as neutral pH. The reproducibility of the titration points included in the calculations was within 0.005 pH units. The pH-metric titrations were performed in the pH range 2.0–12.6. The initial volume of the samples was 10.0 or 20.0 mL. The ligand concentration was in the range 1–2 mM, and metal-ion/ligand ratios of 1:1–1:10 were used. The accepted fitting of the titration curves was always <0.01 mL. Samples were deoxygenated by bubbling purified argon through them for approximately 10 min prior to the measurements. In the case of Fe^{II} samples, argon overpressure was used when Fe^{II} was added to the samples in tightly closed vessels, which were completely deoxygenated by bubbling a stream of purified argon through them for approximately 20 min prior to workup. Argon was also passed over the solutions during the titrations.

The protonation constants of the ligands were determined with the computer program SUPERQUAD,^[29] and PSEQUAD^[30] was utilized to establish the stoichiometry of the complexes and to calculate the stability constants $[\log \beta(M_p L_q H_r)]$ by using the literature data for Fe^{III} and Ga^{III} hydroxido complexes.^[31,32] The values of $\beta(M_p L_q H_r)$ are defined for the general equilibrium $pM + qL + rH \rightleftharpoons M_p L_q H_r$ as $\beta(M_p L_q H_r) = [M_p L_q H_r]/[M]^p [L]^q [H]^r$ in which M denotes the metal ion and L the completely deprotonated ligand. By using this calibration protocol, the protonation and stability constants that involve $[H^+]$ were obtained and are considered to be K_{mixed} (or practical) constants^[33] and are valid only under the given conditions. The calculations were always made from the experimental titration data measured in the absence of any precipitate in the solution.

Spectrophotometric Measurements: A Hewlett Packard 8452A diode array spectrophotometer was used to record the UV/Vis spectra at intervals of 260–820 nm. The path length was 1 cm. Protonation constants and the individual spectra of the species were calculated by the computer program PSEQUAD.^[30] The spectrophotometric titrations were performed on samples of the pure STSC ligand or with Fe^{III}, Fe^{II}, Ga^{III}, Zn^{II} or Cu^{II}; the concentration of ligand was 0.05 mM in the case of Fe^{III}, Ga^{III} and Zn^{II}, 0.2 mM in presence of Fe^{II} and 1 mM for Cu^{II}; and the metal/ligand ratios were 0:1, 1:1 and 1:2 over the pH range between 2 and 12.6 at an ionic strength of 0.10 M (KCl) in 30% (w/w) DMSO/H₂O at (25.0 ± 0.1) °C. For Fe^{II} samples, spectra were recorded under anaerobic conditions.

Determination of the Distribution Coefficient (D): Values of D for STSC and Triapine were determined by the traditional shake flask method^[34] in *n*-octanol/buffered aqueous solution at pH = 6.0 (MES) and 7.4 (HEPES) at (25.0 ± 0.2) °C. Two parallel experiments were performed for each sample. The ligand was dissolved at 25 μM in the *n*-octanol presaturated aqueous solution of the buffer (0.01 M) at constant ionic strength (0.10 M KCl). The aqueous solutions and *n*-octanol with a 1:1 phase ratio were gently mixed with 360° vertical rotation for 3 h to avoid emulsion formation, and the mixtures were centrifuged at 5000 rpm for 3 min with a temperature-controlled centrifuge (Sanyo) at 25 °C. After separation, UV/Vis spectra of the ligand in the aqueous phase were compared with those of the original aqueous solutions in the range 240–440 nm, and D values were calculated as the mean of [absorbance(original solution)/absorbance(aqueous phase after separation) – 1] obtained in the region of $\lambda_{\text{max}} = (320 \pm 10)$ nm. The partition coefficient (P) of STSC is equal to the $D_{6.0}$ value, whereas P of Triapine is equal

to its $D_{7.4}$ if one takes into account the protonation processes of the ligands.

Spectrofluorimetric Measurements: The pH-dependent fluorescence measurements were carried out with a Hitachi-4500 spectrofluorimeter with excitation at 320/390 nm for samples that contained STSC. The emission spectra were recorded by using 5 nm/5 nm or 10 nm/10 nm slit widths in a 1 cm quartz cell in the pH range between 2 and 12.5 in 30% (w/w) DMSO/H₂O (or water) at (25.0 ± 0.1) °C. Samples contained 0.005 mM STSC alone or STSC with 0.0025 mM Ga^{III} or 0.005 mM Zn^{II} at 0.10 M (KCl) ionic strength. Three-dimensional spectra were recorded at 210–550 nm excitations and at 220–650 nm emission wavelengths for the Ga^{III}, Zn^{II} and the sample that contained 0.005 mM STSC at metal-to-ligand ratios of 0:1, 1:1 or 1:2 at neutral and acidic pH by using 5 nm/5 nm slit widths.

¹H NMR Spectroscopic Measurements: ¹H NMR spectroscopic studies were carried out with a Bruker Ultrashield 500 Plus instrument. STSC was dissolved in a 30% (w/w) [D₆]DMSO/D₂O mixture in a concentration of 1.4–2 mM and the Ga^{III} or Zn^{II}/ligand ratios were 0:1; 1:1 and 1:2. The direct pH-meter readings (pH*) were obtained by the pH meter calibrated to the 30% (w/w) DMSO/H₂O according to Irving et al.^[27] and were converted to pH by the following equation: $pH = pH^* + 0.4$.

EPR Measurements and Deconvolution of the Spectra: All continuous-wave (CW) EPR spectra were recorded with a Bruker EleXsys E500 spectrometer (microwave frequency 9.81 GHz, microwave power 10 mW, modulation amplitude 5 G, modulation frequency 100 kHz). During a titration, the isotropic EPR spectra were recorded at room temperature in a circulating system. Ten EPR spectra were recorded at a concentration of 0.5 mM of CuCl₂ and 1 mM ligand between pH = 2.4 and 12.2 and four spectra at concentrations of 1 mM of CuCl₂ and 1 mM ligand between pH = 2.3 and 5.4 in 30% (w/w) DMSO/H₂O, $I = 0.10$ M (KCl). In the latter case, precipitation occurred at higher pH. KOH solution was added to the stock solution to change the pH, which was measured with a Radiometer PHM240 pH/ion meter equipped with a Metrohm 6.0234.100 glass electrode. A Heidolph Pumpdrive 5101 peristaltic pump was used to circulate the solution from the titration pot through a capillary tube into the cavity of the instrument. The titrations were carried out under argon. At various pH values, samples of 0.10 mL were taken and frozen in liquid nitrogen, and the CW-EPR spectra were recorded under the same instrumental conditions as the room-temperature spectra described above. The series of room-temperature CW-EPR spectra were simulated simultaneously by the “two-dimensional” method by using the 2D_EPR program.^[35] Each component curve was described by the isotropic EPR parameters g_o , A_o^{Cu} copper hyperfine and A_o^{N} nitrogen hyperfine couplings and the relaxation parameters α , β and γ , which define the line widths in the equation $\sigma_{M_I} = \alpha + \beta M_I + \gamma M_I^2$, in which M_I denotes the magnetic quantum number of the copper nucleus. The concentrations of the complexes were varied by fitting their formation constants $\beta(M_p L_q H_r)$ defined by the general equilibrium found in the section on pH-potentiometric studies. For each spectrum, the noise-corrected regression parameter (R_j for the *j*th spectrum) is derived from the average square deviation (SQD) between the experimental and the calculated intensities. For the series of spectra, the fit is characterized by the overall regression coefficient R , calculated from the overall average SQD. The details of the statistical analysis were published previously.^[36] The anisotropic spectra were analyzed individually with the EPR program,^[36] which gives the anisotropic EPR parameters ($g_x, g_y, g_z, A_x^{\text{Cu}}, A_y^{\text{Cu}}, A_z^{\text{Cu}}, A_x^{\text{N}}, A_y^{\text{N}}, A_z^{\text{N}}$, and the orientation-dependent line-width parameters).

The spectra were calculated as the sum of the spectra of ^{63}Cu and ^{65}Cu weighted by their natural abundances. The quality of fit was characterized by the noise-corrected regression parameter R_f as above. The copper and nitrogen coupling constants and the relaxation parameters were obtained in field units (Gauss = 10^{-4} T).

Crystallographic Structure Determination: The X-ray-diffraction-quality crystals were obtained by slow concentration of a 3:1 ethanol/water solution that contained $\text{Zn}(\text{OAc})_2$ (1 equiv.) and STSC (4 equiv.; the same structure was obtained in a 1:2 metal/ligand ratio). X-ray diffraction measurements were performed with a Bruker X8 APEXII CCD diffractometer. A single crystal of suitable size was coated with Paratone-N oil, mounted at room temperature on a cryo loop and cooled under a stream of cold N_2 maintained with a Kryoflex low-temperature apparatus. The crystal was positioned at 35 mm from the detector, and 907 frames were measured, each for 10 s over 1° scan width. The data were processed by using SAINT software.^[37] The structure was solved by direct methods and refined by full-matrix least-squares techniques. Non-hydrogen atoms were refined with anisotropic displacement parameters, with the exception of co-crystallized ethanol (0.65 mol-equiv.), which was found to be disordered over three positions. Hydrogen atoms were placed at calculated positions and refined as riding atoms in the subsequent least-squares model refinements. Disorder over two positions was found in the thiosemicarbazone ligand L^{2-} for the sulfur and oxygen atom of the coordinated ethanol and coordinated acetate with values 0.50:0.50, 0.50:0.50 and 0.27:0.23, respectively. The disorder was resolved with constrained anisotropic displacement parameters and restrained bond lengths by using the EADP and SADI instructions of SHELX97. DFIX restrains were used for resolving disorder in the co-crystallized ethanol. The isotropic thermal parameters were estimated to be 1.2 times the values of the equivalent isotropic thermal parameters of the atoms to which hydrogen atoms were bound. The following software programs and computer were used: structure solution, SHELXS-97;^[38] refinement, SHELXL-97;^[38] molecular diagrams, ORTEP;^[39] computer: Intel CoreDuo. Crystal data and structure refinement details for $[\text{Zn}_2(\text{HL})(\text{L})(\text{OAc})\text{EtOH}]\cdot\text{H}_2\text{O}\cdot 0.65\text{EtOH}$ are given in Table S2 in the Supporting Information.

Supporting Information (see footnote on the first page of this article): Concentration distribution curves, UV/Vis spectra, tables with stability constants and crystal data.

Acknowledgments

We thank Prof. Vladimir B. Arion for X-ray data refinement. This work has been supported by the Hungarian Research Foundation OTKA (K77833, K72781), the Hungarian-Austrian Action Foundation and Creating the Center of Excellence at the University of Szeged (TAMOP-4.2.1/B-09/1/KONV-2010-0005). E. A. E. gratefully acknowledges the financial support of Bolyai J. research fellowships and C. R. K the Austrian Science Fund (FWF) (grant P22072).

- [1] a) D. X. West, S. B. Padhye, P. B. Sonawane, *Struct. Bonding (Berlin)* **1991**, *76*, 1–50; b) J. J. Knox, S. J. Hotte, C. Kollmannsberger, E. Winquist, B. Fisher, E. A. Eisenhauer, *Invest. New Drugs* **2007**, *25*, 471–477.
- [2] a) C. M. Nutting, C. M. L van Herpen, A. B. Miah, S. A. Bhide, J. P. Machiels, J. Buter, C. Kelly, D. de Raucourt, K. J. Harrington, *Ann. Oncol.* **2009**, *20*, 1275–1279; b) J. Kolesar, R. C. Brundage, M. Pomplum, D. Alberti, K. Holen, A. Traynor, P. Ivy, G. Wilding, *Cancer Chemother. Pharmacol.*

- 2011**, *67*, 393–400; A. B. Miah, K. J. Harrington, C. M. Nutting, *Eur. J. Clin. Med. Oncol.* **2010**, *2*, 87–92.
- [3] a) J. Shao, B. Zhou, A. J. Di Bilio, L. Zhu, T. Wang, C. Qi, J. Shih, Y. Yen, *Mol. Cancer Ther.* **2006**, *5*, 586–592; b) A. Popovic-Bijelic, C. R. Kowol, M. E. S. Lind, J. Luo, F. Himo, E. A. Enyedy, V. B. Arion, A. Gräslund, *J. Inorg. Biochem.* **2011**, *105*, 1422–1431.
- [4] C. R. Kowol, R. Trondl, P. Heffeter, V. B. Arion, M. A. Jakupiec, A. Roller, M. Galanski, W. Berger, B. K. Keppler, *J. Med. Chem.* **2009**, *52*, 5032–5043.
- [5] a) D. R. Richardson, P. C. Sharpe, D. B. Lovejoy, D. Senatnatne, D. S. Kalinowski, M. Islam, P. V. Bernhardt, *J. Med. Chem.* **2006**, *49*, 6510–6521; b) C. R. Kowol, E. Reisner, I. Chiorescu, V. B. Arion, M. Galanski, D. V. Deubel, B. K. Keppler, *Inorg. Chem.* **2008**, *47*, 11032–11047; c) D. R. Richardson, D. S. Kalinowski, V. Richardson, P. C. Sharpe, D. B. Lovejoy, M. Islam, P. V. Bernhardt, *J. Med. Chem.* **2009**, *52*, 1459–1470.
- [6] E. A. Enyedy, M. F. Primik, C. R. Kowol, V. B. Arion, T. Kiss, B. K. Keppler, *Dalton Trans.* **2011**, *40*, 5895–5905.
- [7] a) D. X. West, A. E. Liberta, S. B. Padhye, R. C. Chikate, P. B. Sonawane, A. S. Kumbhar, R. G. Yerande, *Coord. Chem. Rev.* **1993**, *123*, 49–71; b) S. Padhye, G. B. Kaufmann, *Coord. Chem. Rev.* **1985**, *63*, 127–160.
- [8] E. A. Enyedy, N. V. Nagy, E. Zsigó, C. R. Kowol, V. B. Arion, B. K. Keppler, T. Kiss, *Eur. J. Inorg. Chem.* **2010**, *11*, 1717–1728.
- [9] a) T. S. Lobana, P. Kumari, G. Hundal, R. J. Butcher, *Polyhedron* **2010**, *29*, 1130–1136, N. A. Mangalam, M. R. P. Kurup, *Spectrochim. Acta Part A* **2009**, *71*, 2040–2044.
- [10] a) P. Chellan, T. Stringer, A. Shokar, P. J. Dornbush, G. Vasquez-Anaya, K. M. Land, K. Chibale, G. S. Smith, *J. Inorg. Biochem.* **2011**, *105*, 1562–1568; b) E. Ramachandran, P. Kalaviani, R. Prabhakaran, N. P. Rath, S. Brinda, P. Poornima, V. V. Padma, K. Natarajan, *Metallomics* **2012**, *4*, 218–227; c) P. Kalaviani, R. Prabhakaran, F. Dallemer, P. Poornima, E. Vaishnavi, E. Ramachandran, V. V. Padma, R. Renganathan, K. Natarajan, *Metallomics* **2012**, *4*, 101–113.
- [11] a) S. Laly, G. Parameswaran, *Thermochim. Acta* **1990**, *168*, 43–51; b) D. X. West, M. M. Salberg, G. A. Bain, A. E. Liberta, J. V. Valdes-Martinez, S. Hernandez Ortega, *Transition Met. Chem.* **1996**, *21*, 206–212.
- [12] A. Gulea, D. Poirier, J. Roy, V. Stavila, I. Bulimestru, V. Tapcov, M. Birca, L. Popovschi, *J. Enzyme Inhib. Med. Chem.* **2008**, *23*, 806–818.
- [13] S. M. E. Khalil, M. Shebl, F. S. Al-Gohani, *Acta Chim. Slov.* **2010**, *57*, 716–725.
- [14] I. Dilovic, M. Rubcic, V. Vrdoljak, S. K. Pavelic, M. Kralj, I. Piantanida, M. Cindric, *Bioorg. Med. Chem.* **2008**, *16*, 5189–5198.
- [15] N. S. Reddy, D. V. Reddy, *Microchem. J.* **1985**, *31*, 318–321.
- [16] D. Chattopadhyay, S. K. Mazumdar, T. Banerjee, S. Ghosh, T. C. W. Mak, *Acta Crystallogr., Sect. C* **1988**, *44*, 1025–1028.
- [17] P. Novak, K. Pičuljan, T. Hrenar, V. Smrečki, *Croat. Chem. Acta* **2009**, *82*, 477–483.
- [18] A. A. El-Asmy, O. A. El-Gammal, H. S. Saleh, *Spectrochim. Acta Part A* **2008**, *71*, 39–44.
- [19] N. A. Izmailov, *Electrochemistry of Solutions*, 2nd ed., Khimia, Moscow, **1966**.
- [20] M. B. Ferrari, S. Capacchi, G. Pelosi, G. Reffo, P. Tarasconi, R. Albertini, S. Pinelli, P. Lunghi, *Inorg. Chim. Acta* **1999**, *286*, 134–141.
- [21] a) J. Valdés-Martínez, R. A. Toscano, A. Zentella-Dehesa, M. M. Salberg, G. A. Bain, D. X. West, *Polyhedron* **1996**, *15*, 427–431; b) S. Sen, S. Shit, S. Mitra, S. R. Batten, *Struct. Chem.* **2008**, *19*, 137–142.
- [22] R. Gil-García, R. Zichner, V. Díez-Gómez, B. Donnadiou, G. Madariaga, M. Insausti, L. Lezama, P. Vitoria, M. R. Pedrosa, J. García-Tojal, *Eur. J. Inorg. Chem.* **2010**, *28*, 4513–4525.

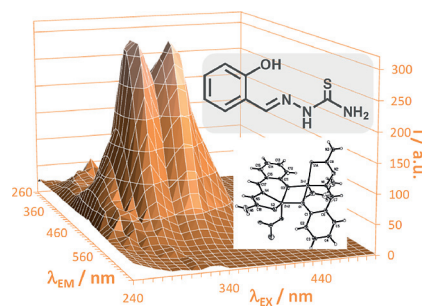
FULL PAPER

- [23] a) K. W. Tan, C. H. Ng, M. J. Maah, S. W. Ng, *Acta Crystallogr., Sect. E* **2009**, *65*, m549; b) K. W. Tan, C. H. Ng, M. J. Maaha, S. W. Ng, *Acta Crystallogr., Sect. E* **2010**, *66*, m569.
- [24] W. S. Wu, Y.-L. Feng, *Z. Kristallogr.* **2003**, *218*, 529–530.
- [25] a) N. A. Ryabova, V. I. Ponomarev, L. O. Atovmyan, V. V. Zelentsov, V. I. Shipilov, *Coord. Chem.* **1978**, *4*, 119; b) N. A. Ryabova, V. I. Ponomarev, V. V. Zelentsov, L. O. Atovmyan, *Crystallogr. Rep.* **1982**, *27*, 279; c) S. Floquet, N. Guillou, P. Negrier, E. Riviere, M. L. Boillot, *New J. Chem.* **2006**, *30*, 1621–1627.
- [26] G. Gran, *Acta Chem. Scand.* **1950**, *4*, 559–577.
- [27] H. M. Irving, M. G. Miles, L. D. Pettit, *Anal. Chim. Acta* **1967**, *38*, 475–488.
- [28] *SCQuery, The IUPAC Stability Constants Database*, Academic Software, Version 5.5, Royal Society of Chemistry, Sourby Old Farm, Timble, Otley, Yorks, **1993–2005**.
- [29] A. Sabatini, A. Vacca, P. Gans, *Talanta* **1974**, *21*, 53–77.
- [30] L. Zékány, I. Nagypál, in: *Computational Methods for the Determination of Stability Constants* (Ed.: D. L. Leggett), Plenum Press, New York, **1985**, pp. 291–353.
- [31] C. F. Baes, R. E. Mesmer, *The Hydrolysis of Cations*, Wiley, New York, **1976**.
- [32] E. Farkas, E. Kozma, T. Kiss, I. Toth, B. Kurzak, *J. Chem. Soc., Dalton Trans.* **1995**, 477–481.
- [33] H. Sigel, A. D. Zuberbühler, O. Yamauchi, *Anal. Chim. Acta* **1991**, *255*, 63–72.
- [34] S. K. Poole, C. F. Poole, *J. Chromatogr. B* **2003**, *797*, 3–19.
- [35] A. Rockenbauer, T. Szabó-Plánka, Zs. Árkosi, L. Korecz, *J. Am. Chem. Soc.* **2001**, *123*, 7646–7654.
- [36] A. Rockenbauer, L. Korecz, *Appl. Magn. Reson.* **1996**, *10*, 29–43.
- [37] *SAINT-Plus*, Version 7.68a, and *APEX2*, Bruker-Nonius AXS Inc., **2008**, Madison, Wisconsin, USA.
- [38] G. M. Sheldrick, *Acta Crystallogr., Sect. A* **2008**, *64*, 112–122.
- [39] M. N. Burnett, G. K. Johnson, *ORTEP III*, Report ORNL-6895, Oak Ridge National Laboratory, Oak Ridge, TN, **1996**.

Received: April 11, 2012


Published Online: ■

The stability and stoichiometry of salicylaldehyde thiosemicarbazone complexes formed with various metal ions have been studied by means of pH potentiometry in partially aqueous solution combined with UV/Vis, EPR, ^1H NMR spectroscopy and fluorimetry. Speciations are compared to those of analogous $\alpha(N)$ -pyridyl thiosemicarbazones.



(Thiosemicarbazone)metal Complexes

É. A. Enyedy,* É. Zsigó, N. V. Nagy,
C. R. Kowol, A. Roller, B. K. Keppler,
T. Kiss 1–13

Complex-Formation Ability of Salicylaldehyde Thiosemicarbazone towards Zn^{II} , Cu^{II} , Fe^{II} , Fe^{III} and Ga^{III} Ions 

Keywords: Solution equilibrium / Stability constants / Thiosemicarbazones / Antitumor agents / EPR spectroscopy